Engineered Nanomaterial Exposure: Effects on Epigenetic and MiRNA Regulation of Cardiac Mitochondria

Q. A. Hathaway[1], C. E. Nichols[2], D. L. Shepherd[1], A. J. Durr[1], P. A. Stapleton[3], A. B. Abukabda[1], T. R. Nurkiewicz[1], and J. M. Hollander[1]
[1]West Virginia University, Morgantown, WV, [2]NIEHS, Durham, NC, and [3]Rutgers, The State University of New Jersey, Piscataway, NJ

ABSTRACT

Continuing to understand the toxicological implications of engineered nanomaterials (ENM) becomes increasingly important as the incidence of exposure for the producer, and consumer, rises. Pulmonary exposure to ENMs have revealed a myriad of systemic physiological alterations, including decreased microvascular reactivity, increased inflammation, and ENM translocation. Of importance, cardiac function is detrimentally impacted after ENM inhalation exposure.

Conventional measures of echocardiography following ENM exposure (aerodynamic diameter D_p = 131.6 nm) in adult mice (8-12 weeks old) revealed an increased E/A ratio and mitral valve deceleration time (P < 0.05 for both), suggestive of diastolic dysfunction. Also, stress-strain analyses displayed deviations in strain parameters, including a 3-fold increase in radial strain and overall increase in radial strain rate (P < 0.05 for both), indicative of a restrictive filling pattern. A potential cause of this dysfunction may be related to mitochondrial function, which has displayed a decrease in State 3 respiration rate (P < 0.05). However, the direct mechanisms impacting cardiac functional alterations and decreased mitochondrial function have not fully been elucidated.

Examination of mRNA and epigenetic chromatin modifications (H3K4me3 and H3K27me3) in fetal progeny following maternal exposure revealed changes in the genetic expression of microRNA encoding genes. Specifically, the gene Ppargc1b (which encodes microRNA-378a, a target of mitochondrial transcribed ATP6) did not exhibit a transcriptional change but binding of the open chromatin modification H3K4me3 was significantly increased, suggesting epigenetic activation of the locus. In adult mice, microRNA-378a-3p is found to be increased (4.62 fold, P = 0.015) in the cytoplasm after ENM exposure.

How microRNA expression in the cytoplasm and mitochondria change, and the extent of epigenetic regulation involved, could help to better elucidate the molecular processes behind the cardiac functional deficits exhibited after ENM exposure.

CONTACT

Quincy A. Hathaway
West Virginia University

INTRODUCTION

The advent and advancement of nanotechnology has continued to drive utilization and adaptation of engineered nanomaterials (ENMs) in consumer goods (Besinis et al. 2015; Diez-Pascual and Diez-Vicente 2015; Dong et al. 2014; Giese et al. 2018), with nano-TiO_2 becoming one of the most prolifically implemented ENMs (Gottschalk et al. 2015; Hendren et al. 2011). While the beneficial manufacturing properties of ENMs are clear, the rate of application in new products and devices outpaces our understanding of the toxicology of these materials. Though progress has been made regarding the pathological consequences on organ systems and the physiological impact of ENM exposure, the molecular mechanisms governing their toxicity are at best, poorly defined. Systemic health effects following ENM exposure are linked to mitochondrial dysfunction, not only in the lungs (Li et al. 2016; Ruenraroengsak and Tetley 2015) but also in the cardiovascular system (Hathaway et al. 2017a; Nichols et al. 2018; Stapleton et al. 2015). The heart has been established as a significant contributor to the overall pathophysiological outcomes elicited by ENM exposure (Holland et al. 2016; Kan et al. 2012; Li et al. 2007; Sotiriou et al. 2012; Stapleton et al. 2012). Cardiac mitochondrial function is crucial in maintaining/restoring cardiac homeostasis after ENM insult, as it is a central determinant of metabolic and bioenergetic capacity.

MicroRNAs (MiRNAs) are transcribed as pri-miRNA species within the nucleus (processed through Drosha) and travel to the cytoplasm as pre-miRNA (processed through Dicer) where they eventually assume their mature miRNA conformation (Gulyaeva and Kushlinskiy 2016; Shukla et al. 2011). These small non-coding RNA species (~22 nt) that originate in both intragenic and intergenic regions of the genome are known to individually function in regulating multiple genetic and epigenetic pathways (Lai et al. 2016; Sato et al. 2011). The manipulation of a miRNA that controls metabolic and mitochondrial function provides a potentially novel therapeutic strategy for controlling cellular insults precipitated by ENM exposure. In the heart, and other mitochondrial dense tissue, peroxisome proliferator-activated receptor gamma coactivator 1-beta (Ppargc1b or PCG-1β) is highly expressed (Esterbauer et al. 1999), and is central in the control of metabolism (Carrer et al. 2012; Lelliott et al. 2006; Vianna et al. 2006). MiRNA-378a, which encodes both the 3p and 5p mature variants, resides within the first intron of PCG-1β gene.

The objective of the current study was to determine whether manipulation of miRNA-378a expression could alter adverse cardiovascular and metabolic outcomes associated with ENM exposure. Our findings indicate that knockout, and knockdown to a lesser extent, of miRNA-378a improves cardiac and mitochondrial function by altering global bioenergetic and respiration capacity following nano-TiO_2 exposure. This is the first study to determine the impact of altered miRNA expression on the response to ENM exposure *in vivo*.

Figure 1

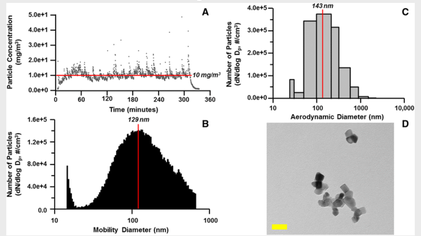

Figure 1: Maternal nano-TiO_2 exposure particle characterization for RNA sequencing experiments. **a** Total aerosol concentration (10 mg/m^3) of engineered nano-TiO_2 during maternal exposures. **b** Nano-TiO_2 size distribution (mobility diameter, 129.4 nm) using a scanning mobility particle sizer (SMPS). **c** Nano-TiO_2 size distribution (aerodynamic diameter, 143.3 nm) using an electrical low-pressure impactor (ELPI). (D) Transmission electron microscopy image of aerosolized nano-TiO_2 collected via a sampling filter during an exposure

METHODS AND MATERIALS

MiRNA-378a Knockout Mouse Model

The animal model have been previously published (Carrer et al. 2012). Briefly, miRNA-378a is located within the first intron of the peroxisome proliferator-activated receptor gamma coactivator 1-beta gene (Ppargc1b or PGC-1β). MiRNA-378a was removed in knockout animals, preserving the function of PGC-1β.

Nano-TiO_2 Inhalation Exposures

Male and female wild-type (WT), heterozygous for miRNA-378a knockout (Het), and complete miRNA-378a knockout (KO) FVB mice were used. Nano-TiO_2 P25 powder, purchased from Evonik (Aeroxide TiO2, Parsippany, NJ)), was prepared through drying, sieving, and storing, as previously described (Knuckles et al. 2012; Nurkiewicz et al. 2008), and was composed of anatase (80%) and rutile (20%) TiO_2. Nano-TiO_2 inhalation involved whole-body exposure through the use of an aerosol generator (US Patent No. 8,881,997) as previously described (Nurkiewicz et al. 2008; Sager et al. 2008).

Echocardiography

Ultrasound imaging was performed on mice 24 hours following exposure. M-mode, B-Mode, and PW Doppler imaging acquisition and analysis have been previously described by our laboratory (Hathaway et al. 2017a; Nichols et al. 2015; Nichols et al. 2018). In both the short and long axis visualizing the LV, B-Mode images were used for speckle-tracking-based strain analyses. The procedure for speckle-tracking-based strain analysis have been previously described by our laboratory (Shepherd et al. 2016).

Mitochondrial Respiration

State 3 and state 4 respiration rates were analyzed in isolated mitochondria as previously described (Croston et al. 2014; Thapa et al. 2015) with adaptations. To measure oxygen consumption of mitochondria, a multi-unit (8 channel) Oxytherm Peltier Electrode apparatus (Hansatech Instruments, Norfolk, England) was utilized. Maximal complex I-mediated respiration was initiated by the addition of glutamate (5 mM) and malate (5 mM) for glucose mediated pathways or palmitoyl-carnitine (50 μM) and malate (5mM) for fatty-acid mediated pathways. Data for state 3 (250mM ADP) and state 4 (ADP-limited) respiration were expressed as nmol of oxygen consumed/mL/min, standardized to protein concentration.

Electron Transport Chain Complex Activities

Maximal activity for electron transport chain (ETC) complexes I, III, IV and V (ATP synthase) were measured as previously described (Hathaway et al. 2017a).

Quantitative PCR

RNA was isolated from 20 mg of cardiac, lung, and liver tissue or from isolated cardiac mitochondria, using the miRNeasy Mini Kit (product no.: 217004, Qiagen, Hilden, Germany). RNA was converted to cDNA with the First-strand cDNA Synthesis kit for miRNA (product no.: HP100042, Origene, Rockville, MD). Experiments were performed on the Applied Biosystems 7900HT Fast Real-Time PCR system (Applied Biosystems, Foster City, CA)

Western Blot Analyses

Immunoblotting was performed on 4 –12% gradient gels through MES SDS-PAGE, as previously described (Nichols et al. 2015; Thapa et al. 2015). Standardization was determined through GAPDH expression. Data were captured using GeneSnap/GeneTools software (Syngene). Densitometry was analyzed using Image J Software (NIH, Bethesda, MD). All values were expressed as optical density with arbitrary units.

Statistics

Significance was determined using either a two-tailed Student's t-test or one-way analysis of variance (ANOVA), where appropriate. Tukey's multiple comparisons test was implemented following the ANOVA to derive significance between multiple groups. Differences between groups were considered statistically different ($P \leq 0.05$, denoted by *, and $P \leq 0.01$, denoted by **). All data are presented as the mean ± standard error of the mean (SEM).

Figure 2

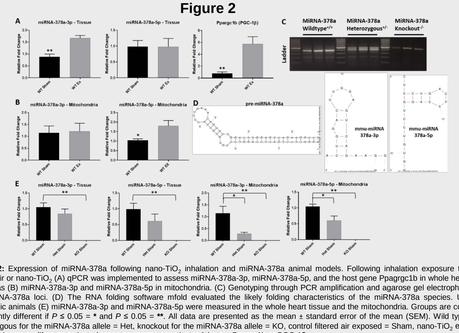

Figure 2: Expression of miRNA-378a following nano-TiO_2 inhalation and miRNA-378a animal models. Following inhalation exposure to control filtered air or nano-TiO_2 (A) qPCR was implemented to assess miRNA-378a-3p, miRNA-378a-5p, and the host gene Ppargc1b in whole heart tissue as well as (B) miRNA-378a-3p and miRNA-378a-5p in mitochondria. (C) Genotyping through PCR amplification and agarose gel electrophoresis for the miRNA-378a loci. (D) The RNA folding software mfold evaluated the likely folding characteristics of the miRNA-378a species. Using the transgenic animals (E) miRNA-378a-3p and miRNA-378a-5p were measured in the whole heart tissue and the mitochondria. Groups are considered significantly different if $P \leq 0.05$ = * and $P \leq 0.05$ = **. All data are presented as the mean ± standard error of the mean (SEM). Wild type = WT, heterozygous for the miRNA-378a allele = Het, knockout for the miRNA-378a allele = KO, control filtered air exposed = Sham, nano-TiO_2 exposed = Ex, peroxisome proliferator-activated receptor gamma coactivator 1-beta = Ppargc1b or PGC-1β.

RESULTS

Figure 3

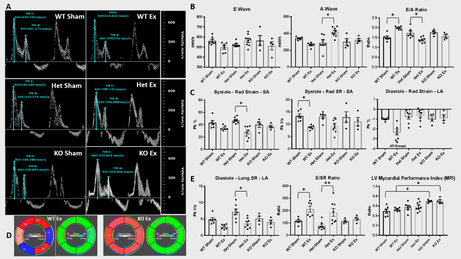

Figure 3: Cardiac function following nano-TiO_2 inhalation exposure. (A) PW Doppler images illustrate changes in E and A wave velocities following exposure. (B) E and A wave velocities, as well as E/A wave ratios, are represented from PW Doppler imaging. Speckle-tracking analyses from B-Mode short and long axis images for (C) systolic and diastolic strain and strain rate. (D) An illustration of dyssynchrony of the endocardium during short axis systolic radial stain (indicated by color) in the WT nano-TiO_2 exposed animals compared to conserved strain parameters in the KO exposed animals. (E) The diastolic longitudinal strain rate coupled with the E wave velocities provided a prognostic cardiac health index for the left ventricle (LV), while the LV myocardial performance index (MPI) further provided a prognostic index of the left ventricular ejection parameters. Groups are considered significantly different if $P \leq 0.05$ = * and $P \leq 0.05$ = **. All data are presented as the mean ± standard error of the mean (SEM). Wild type = WT, heterozygous for the miRNA-378a allele = Het, knockout for the miRNA-378a allele = KO, control filtered air exposed = Sham, nano-TiO_2 exposed = Ex, left ventricular short axis = SA, left ventricular long axis = LA, longitudinal = Long, radial = Rad.

Figure 5

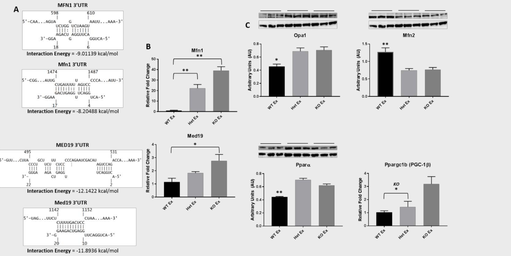

Figure 5: Molecular targets of miRNA-378a. (A) Binding interactions determined for both human (MFN1 and MED19) and mouse (Mfn1 and Med19) using IntaRNA 2.0. Interaction energies are calculated as binding propensity through free energy binding near the seed sequence region. (B) qPCR of Mfn1 and Med19. (C) Immunoblotting and qPCR of targets relating to the miRNA-378a pathway. Groups are considered significantly different if $P \leq 0.05$ = * and $P \leq 0.05$ = **. All data are presented as the mean ± standard error of the mean (SEM). Wild type = WT, heterozygous for the miRNA-378a allele = Het, knockout for the miRNA-378a allele = KO, control filtered air exposed = Sham, nano-TiO_2 exposed = Ex, mitofusin 1 = Mfn1, mediator complex subunit 19 = Med19, 3' untranslated region = 3' UTR, optic atrophy 1 = OPA1, mitofusin 2 = Mfn2, peroxisome proliferator-activated receptor alpha = PPARα, peroxisome proliferator-activated receptor gamma coactivator 1-beta = Ppargc1b or PGC-1β.

Figure 4

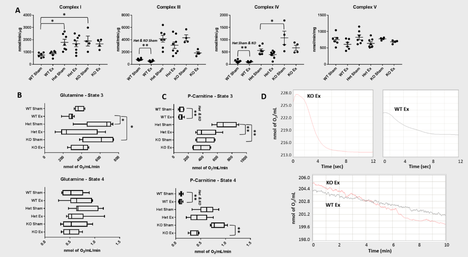

Figure 4: Bioenergetic function of cardiac mitochondria following nano-TiO_2 inhalation exposure. (A) Electron transport chain complex activities were measured for complexes I, III, IV, and V. Mitochondrial State 3 and State 4 respiration were measured through (B) glucose mediated pathways and (C) fatty acid mediated pathways. (D) State 3 and State 4 respiration changes between a representative WT and KO animal illustrates changes in oxygen consumption when using p-carnitine for fatty acid mediated respiration. Groups are considered significantly different if $P \leq 0.05$ = * and $P \leq 0.05$ = **. All data are presented as the mean ± standard error of the mean (SEM). Wild type = WT, heterozygous for the miRNA-378a allele = Het, knockout for the miRNA-378a allele = KO, control filtered air exposed = Sham, nano-TiO_2 exposed = Ex, palmitoyl carnitine = P-Carnitine

Figure 6

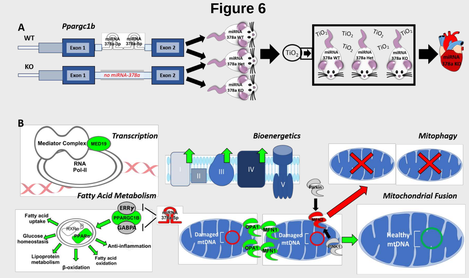

Figure 6: General schema of miRNA-378a interactions following exposure. (A) Transgenic mouse model, illustrating miRNA-378a wild type and knockout alleles. Mice were exposed to a total nano-TiO_2 deposition of 10 mg/m^3. Cardiac issue was excised for subsequent experimental procedures. (B) Molecular changes in the KO nano-TiO_2 exposed heart compared to WT exposed. Med19 was shown to be significantly elevated, an important cofactor in regulating cellular transcription. Metabolically, fatty acid metabolism was elevated, likely through mediators such as Ppara and Ppargc1b. Increased mitochondrial fusion (Mfn1 and Opa1) as well as decreased mitophagy contribute to the integrity of mitochondria following exposure. All of these molecular pathways that are altered with the repression of miRNA-378a contribute to elevated bioenergetics and cardiac function in the KO compared to the WT mice. Wild type = WT, heterozygous for the miRNA-378a allele = Het, knockout for the miRNA-378a allele = KO, mitofusin 1 = Mfn1, mediator complex subunit 19 = Med19, 3' untranslated region = 3' UTR, optic atrophy 1 = OPA1, mitofusin 2 = Mfn2, peroxisome proliferator-activated receptor alpha = PPARα, peroxisome proliferator-activated receptor gamma coactivator 1-beta = Ppargc1b or PGC-1β.

CONCLUSIONS

Understanding the role of miRNAs in regulating the response to ENM inhalation exposure is important in defining the molecular consequences involved in the pathology. In this study, we found that miRNA-378a, a small non-coding RNA, was directly involved in regulating cardiac function following nano-TiO_2 inhalation exposure. The knockout, and to a lesser extent knockdown, of miRNA-378a expression was associated with preserved cardiac function following exposure and increased bioenergetic capacity when compared to WT animals. The mechanisms governing this functional difference are likely through bolstered mitochondrial health, including increased mitochondrial fusion and fatty acid metabolism and decreased mitophagy, as well as changes to cellular transcription. This study investigates for the first time, the *in vivo* role of a miRNA in attenuating cardiovascular consequences following exposure to an ENM, setting miRNA-378a as a potential target for future investigations.

Future Directions

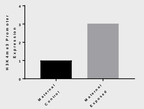

Future Directions: Chromatin Immunoprecipitation (ChIP) Sequencing of H3K4me3 for gestational nano-TiO_2 exposed progeny. Ppargc1b has increased H3K4me3 association at its promoter loci, suggesting increased epigenetic regulation and subsequent expression of the gene. Histone 3 lysine 3 tri-methylation = H3K4me3

Grants

This work was supported by: R01 HL-128485 (JMH), R01-ES015022 (TRN), AHA-17PRE33660333 (QAH), AHA-13PRE16850066 (CEN), NSF-1003907 (TRN), DGE-1144676 (QAH, ABA, TRN), and WV-INBRE support by NIH Grant P20GM103434

Disclosures

The authors declare that they have no competing interests, financial or otherwise.